Comparison of Some Exact and Approximate Results for Gases of Parallel Hard Lines, Squares, and Cubes*

WILLIAM G. HOOVER† AND JACQUES C. POIRIER‡

Department of Chemistry, Duke University, Durham, North Carolina

(Received 16 July 1962)

The first seven virial coefficients for hard parallel lines, squares, and cubes, as derived from approximations of the ring and watermelon type, are compared with the exact coefficients. These approximations give no useful information as to the sign or magnitude of the virial coefficients.

A Cartesian distribution function depending upon only one space coordinate arises naturally for the line, square, and cube molecules. The first four terms of the exact number density expansion of this function are presented and compared with results obtained by iteration from the Percus-Yevick, Kirkwood, and convolution integral equations. The Percus-Yevick equation yields a distribution function which closely resembles the exact result at low densities.

Virial coefficients are obtained from the approximate distribution functions by means of the Ornstein-Zernicke relation and the virial theorem, as well as from a relation between the potential of mean force at zero separation and the virial coefficients. This last relation (which is valid for hard spheres as well as lines, squares, and cubes) has an interesting graphical interpretation and leads to correct values for the third virial coefficient from the Kirkwood equation, but not from the Percus-Yevick or convolution equations.

1. INTRODUCTION

STATISTICAL mechanics provides us with exact expressions for the pressure and radial distribution function in terms of the pairwise-additive intermolecular potential function $\phi(\mathbf{r})$, the volume V, the number of molecules N, and the temperature T.[1] Ordinarily, the integrals involved are impossible to evaluate; however, one can make an exact expansion of the pressure P, or radial distribution function $g(\mathbf{r})$, obtaining expressions useful for small values of the expansion parameter. A number density ($\rho \equiv N/V$) expansion is often used and leads to the following exact expansions[1,2] for the pressure and radial distribution function:

$$P/kT = \sum_{n=1} B_n \rho^n, \tag{1}$$

$$\exp[\phi(\mathbf{r})/kT] g(\mathbf{r}) = \sum_{n=0} g_n(\mathbf{r}) \rho^n \equiv \mathcal{G}(\mathbf{r}). \tag{2}$$

The B_n and $g_n(\mathbf{r})$ are sums of integrals over the coordinates of n molecules. The integrands, best expressed graphically, are complicated functions of the temperature and intermolecular potential. In particular, from work due largely to Mayer, we know that[3]

$$B_1 \equiv 1, \quad B_{n>1} = \frac{1-n}{n!V} \sum_{i=1}^{S(n)} \int \mathfrak{g}_i S_i(n)\, d\mathbf{r}_1 \cdots d\mathbf{r}_n, \tag{3}$$

$$g_0 \equiv 1, \quad g_{n>0}(\mathbf{r}) = \frac{1}{n!} \sum_{i=1}^{S^*(n+2)} \int \mathfrak{g}_i^* S_i^*(n+2)\, d\mathbf{r}_3 \cdots d\mathbf{r}_{n+2}.[4] \tag{4}$$

The $S_i(n)$ in (3) are all possible types of *stars* (for a list of all graphical terms used in this paper, together with their definitions, the reader is referred to Appendix I; we consistently italicize all graphical terms.) which can be constructed with n *unlabeled points* and up to $\binom{n}{2} \equiv n(n-1)/2$ *lines*. The $S_i^*(n)$ in (4) are all possible types of *doubly rooted graphs*, with $n-2$ *unlabeled points* and *root points* labeled 1 and 2, which would become or remain *stars* if the *line* joining the *root points* were added to the *doubly rooted graphs*. $S(n)$ and $S^*(n)$ are, respectively, the number of types of *stars* of n *unlabeled points* and the number of *doubly rooted graphs* of $n-2$ *unlabeled points* and two specially designated *root points*. The $\mathfrak{g}_i$ and $\mathfrak{g}_i^*$ are the number of

* This work was supported by a grant from the Alfred P. Sloan Foundation.

† Present address: Lawrence Radiation Laboratory, Livermore, California.

‡ Alfred P. Sloan Foundation Fellow.

[1] See, for example, J. de Boer, Repts. Progr. Phys. **12**, 305 (1949).

[2] J. E. Mayer and M. G. Mayer, *Statistical Mechanics* (John Wiley & Sons, Inc., New York, 1940), Chap. 13.

[3] See references 1 and 2 as well as M. Born and K. Fuchs, Proc. Roy. Soc. (London) A166, 391 (1938); B. Kahn and G. E. Uhlenbeck, Physica 5, 399 (1938).

[4] In general, we use $\mathbf{r}$ as the argument of an angle-dependent function, and r as the argument of a function of one space coordinate only. We call $g(\mathbf{r})$ the "radial distribution function" in this paper; for the potentials which we use, $g(\mathbf{r})$ depends upon both angle and distance. The function $\mathcal{G}(\mathbf{r})$ introduced in (2) is, for the potentials which we use, identical with $g(\mathbf{r})$ for $\phi(\mathbf{r}) = 0$ ($\mathbf{r}$ large), but finite and nonzero, unlike $g(\mathbf{r})$, for $\phi(\mathbf{r}) = \infty$ ($\mathbf{r}$ small). $\mathcal{G}(\mathbf{r})$ may be thought of as a "radial distribution function" for two particles which interact normally with particles 3...N, but not with each other [$\phi(\mathbf{r}_{12}) \equiv 0$].

TABLE I. The number of stars of J junctions and n unlabeled points.

J	0	2	3	4	5	6	7
$n=2$	1	0	0	0	0	0	0
$n=3$	1	0	0	0	0	0	0
$n=4$	1	1	0	1	0	0	0
$n=5$	1	3	1	2	3	0	0
$n=6$	1	6	5	13	12	19	0
$n=7$	1	10	18	54	94	142	149

ways a particular S_i or S_i^* may be labeled. The *lines* in the *graph* represent Mayer f functions, $f(\mathbf{r})\equiv \exp[-\phi(\mathbf{r})/kT]-1$. A list of the S_i through $S_i(7)$ and S_i^* through $S_i^*(5)$ is available.[5]

Recently many approximate theories have been developed[6–10] with the hope of getting values of P and $g(\mathbf{r})$ at lower temperatures or higher densities than can conveniently be treated by the exact expansions (1) and (2). For simple potentials one can generally express the results of the approximate theories as power series in ρ, and make a term-by-term comparison with (1) and (2). For realistic potentials it has proved difficult to generate more than two or three terms of (1) and (2). Therefore, the approximate results can only be compared with experiment (in which case the cause of disagreement is difficult to isolate) or with direct Monte Carlo[11] or molecular dynamics[12] studies. The hard cube potential,[13] which sacrifices considerable realism in order to simplify calculations, allows comparisons to be made at relatively high densities because the B_n for $n<8$ and the $g_n(\mathbf{r})$ for $n<4$ are known exactly.[13–15] It is the purpose of this paper to use the Hoover–De Rocco results (and those of Geilikman and Zwanzig) in a comparison of some exact and approximate results for this potential. We wish to stress that throughout this paper the terms lines (not italicized), squares, and cubes refer to molecules with (i) molecular volumes of σ, σ^2, and σ^3, respectively (we often set $\sigma\equiv 1$ for convenience in writing results); (ii) a potential energy which is infinite on overlap, and zero otherwise; and (iii) an orientation parallel to a fixed Cartesian coordinate system.

In Sec. 2 we compare the virial coefficients calculated by means of Abe's *junction* expansion method[6] with the exact B_n. In Sec. 3 we compare the $g_n(\mathbf{r})$ functions from the Percus–Yevick,[7] Kirkwood,[8] and convolution[9] integral equations with the exact $g_n(\mathbf{r})$. In Sec. 4 we use these functions in a calculation and comparison of virial coefficients derived with the help of (i) the Ornstein–Zernicke relation,[16] (ii) the virial theorem,[17] and (iii) our new relation[18] between the potential of mean force at zero separation and the virial coefficients. In Sec. 5 we discuss the conclusions and speculations to which our results lead.

2. APPROXIMATIONS BASED ON GRAPH TYPE

A group of approximate theories for the pressure is characterized by the inclusion of only certain types of *stars* [from the total of $S(n)$ types] followed by a summation over n. For example, as shown by Montroll and Mayer,[19] the contribution of all *ring graphs* (—, △, □, ⬠, ⋯) to the pressure can be calculated with the help of Fourier transforms. More recently Abe[6] has pointed out that the nth virial coefficient B_n may be written as a sum of contributions $B(j,n)$ from the *stars* of 0, 2, 3, ⋯j, ⋯n *junctions*:

$$B_n=\sum_{j=0}^{n}B(j,n); \qquad (5)$$

$j=1$ is omitted because a *star* cannot have exactly one

[5] W. G. Hoover and A. G. De Rocco, J. Chem. Phys. **36**, 3141 (1962).
[6] R. Abe, J. Phys. Soc. Japan **14**, 10 (1959).
[7] J. K. Percus and G. J. Yevick, Phys. Rev. **110**, 1 (1958).
[8] J. G. Kirkwood, J. Chem. Phys. **3**, 300 (1935).
[9] E. Meeron and E. R. Rodemich, Phys. Fluids **1**, 246 (1958); E. Meeron, J. Math. Phys. **1**, 192 (1960); Physica **26**, 445 (1960); Progr. Theoret. Phys. (Kyoto) **24**, 588 (1960); T. Morita and K. Hiroike, Progr. Theoret. Phys. (Kyoto) **23**, 1003 (1960); J. M. J. Van Leeuwen, J. Groenveld, and J. de Boer, Physica **25**, 792 (1959); L. Verlet, Nuovo cimento **18**, 77 (1960).
[10] M. Born and H. S. Green, Proc. Roy. Soc. (London) **A188**, 10 (1946); J. Yvon, *Actualités scientifiques et industrielles* (Hermann & Cie., Paris, 1935), Vol. 203.
[11] N. Metropolis, A. W. Rosenbluth, M. N. Rosenbluth, A. H. Teller, and E. Teller, J. Chem. Phys. **21**, 1087 (1953).
[12] B. J. Alder and T. E. Wainwright, J. Chem. Phys. **31**, 459 (1959).
[13] The hard cube model was introduced by B. T. Geilikman, Proc. Acad. Sci. U.S.S.R. **70**, 25 (1950). Geilikman calculated B_2 and B_3 for this model.
[14] B_4 and B_5 for hard cubes were calculated by R. W. Zwanzig, J. Chem. Phys. **24**, 855 (1956).
[15] B_6 [J. Chem. Phys. **34**, 1059 (1961)] and[5] B_7, as well as $g_1(\mathbf{r})\cdots g_3(\mathbf{r})$, were calculated for hard cubes by W. G. Hoover and A. G. De Rocco.
[16] See reference 1, p. 365.
[17] J. O. Hirschfelder, C. F. Curtiss, and R. B. Bird, *Molecular Theory of Gases and Liquids* (John Wiley & Sons, Inc., New York, 1954), p. 134.
[18] W. G. Hoover and J. C. Poirier, J. Chem. Phys. **37**, 1041 (1962).
[19] E. W. Montroll and J. E. Mayer, J. Chem. Phys. **9**, 626 (1941).

TABLE II. $B_n(J)$ for hard lines. The molecular side length is unit volume.

J	0	2	3	4	5	6	7
$n=2$	1.000	1.000					
$n=3$	1.000	1.000	1.000				
$n=4$	−2.000	1.500	1.500	1.000			
$n=5$	3.833	−12.667	1.833	2.333	1.000		
$n=6$	−7.333	48.500	−38.667	0.292	3.958	1.000	
$n=7$	14.017	−149.825	208.933	−85.733	−8.950	7.233	1.000

junction. The first term in (5) corresponds to the *ring* approximation; the first two terms correspond to the *watermelon* approximation. Abe has shown how one can sum (over n) the additional contribution from the *watermelon graphs* ($j=2$) to the Helmholtz free energy, and hence to the pressure. The convergence of the sum in (5) is of interest. At best, only a few terms in this sum give a good approximation to B_n; at worst, all must be used. Because the values of all of the *star* integrals of less than eight *points* are known[5] for lines, squares, and cubes, it is straightforward, although tedious, to check on the convergence of the sum in (5) for $n<8$ using these simple models. The following procedure was used.

For a particular n, values of the one-dimensional $(1/V)\int S_i(n)d\mathbf{r}_1\cdots d\mathbf{r}_n$ from reference 5 were punched on cards together with the g_i for each *star* and ordered by number of *junctions*. Table I gives the number of *stars* with n *points* and j *junctions* for $n<8$. The Duke IBM 7070 computer then squared and cubed the one-dimensional values, thus getting[5,14,20] the two and three-dimensional $(1/V)\int S_i(n)d\mathbf{r}_1\cdots d\mathbf{r}_n$; multiplied by the g_i and punched out the contribution of each *star* to $\sum(1/V)\int S_i(n)d\mathbf{r}_1\cdots d\mathbf{r}_n$. While adding these contributions the computer printed cumulative totals, from which, on multiplication by $(1-n)/n!$, the $B(j,n)$ were selected. It was necessary to use multiple-precision integer arithmetic to avoid round-off error.

As an illustration we give $B(0,5)+B(2,5)+B(3,5)$ for squares [corresponding to the first three terms in (5) for $n=5$] in (6):

$$B_5(3)\equiv\sum_{j=0}^{3}B(j,5)$$

$$=\frac{1-5}{5!V}\int[12\,\square+60\,\square+10\,\square+10\,\square+60\,\square]dx_1\cdots dy_5. \tag{6}$$

$B_n(J)$ is the value of B_n obtained using all *stars* of n *points* and 0, 2, $\cdots J$ *junctions*. Substituting values for the *star* integrals in (6), and choosing σ^2 as unit volume, we find,

$$B_5(3)=\frac{1-5}{5!}[-12(\tfrac{230}{24})^2+60(\tfrac{196}{24})^2+10(\tfrac{192}{24})^2$$
$$-10(\tfrac{180}{24})^2-60(\tfrac{174}{24})^2]$$
$$=101760/(30\times576)=53/9. \tag{7}$$

In Tables II–IV we present $B_n(J)$ for lines, squares, and cubes. The results are enlightening. They show no convenient way of determining either the sign or magnitude of a particular B_n, even if all of the contributions from *stars* of $n-1$ or fewer *junctions* are known. Leaving out the *stars* of any particular number of *junctions* in (5) gives a very poor approximation to

TABLE III. $B_n(J)$ for hard squares. The molecular area σ^2 is unit volume.

J	0	2	3	4	5	6	7
$n=2$	2.000	2.000					
$n=3$	3.000	3.000	3.000				
$n=4$	−10.667	5.667	5.667	3.667			
$n=5$	36.736	−99.236	5.889	12.472	3.722		
$n=6$	−129.067	699.165	−435.529	−40.492	35.886	3.025	
$n=7$	458.423	−3983.439	4504.145	−1131.915	−412.976	117.715	1.651

[20] In the machine computations and (7) [but not in (6)] the algebraic sign of each *star* integral, which is independent of the dimensionality of the models considered here, is, as in reference 5, conveniently attached to g_i rather than to the integral.

TABLE IV. $B_n(J)$ for hard cubes. The molecular volume σ^3 is unit volume.

J	0	2	3	4	5	6	7
$n=2$	4.000	4.000					
$n=3$	9.000	9.000	9.000				
$n=4$	−56.889	19.333	19.333	11.333			
$n=5$	352.054	−767.330	−5.174	59.868	3.160		
$n=6$	−2271.573	9976.154	−4739.442	857.766	330.338	−18.880	
$n=7$	14992.975	−104731.870	94299.674	−10432.294	−10935.611	1914.669	−43.505

the virial coefficient in question. It is difficult to see how the use of a more realistic potential function would alter this conclusion.

Properties of *star graphs*, other than the number of *junctions*, can be used to order the contributions of the *graphs* to the pressure. Number of *lines*, for example, could be used. We mention this possibility because, for hard lines, squares, and cubes, we can calculate the contributions of all *complete* and *nearly complete graphs* to the pressure. (*Complete graphs* are *stars* of n *points* with the maximum number $\binom{n}{2}$ of *lines*: —, △, ⊠, ⛤, ⋯; by *nearly complete graphs* we mean the *stars* of n *points* with $\binom{n}{2}-1$ *lines*: ⊡, ⛤, ⋯.) In general (see Appendix II) the value of an *n-point complete graph* integral is $(-)^{[n/2]}n^d$, $[(1/V)\int\boxtimes dx_1\cdots dx_4=4$, for example], where d is the dimensionality of the molecules (1 for lines, 2 for squares, and 3 for cubes), [ ] indicates the greatest integer function,[21] and $\sigma\equiv 1$. One can therefore sum the contribution of all such *graphs* to the pressure. In one dimension we get

$$(P/kT)_{\text{lines}}=\rho+\tfrac{1}{2}2\rho^2+\tfrac{1}{3}3\rho^3-\tfrac{1}{8}4\rho^4 -\tfrac{1}{30}5\rho^5+\cdots\equiv\rho+\rho^2(\sin\rho+\cos\rho). \quad (8)$$

For simplicity we have set the side length of the molecules equal to unit distance. In two and three dimensions the results analogous to (8) are

$$(P/kT)_{\text{squares}}=\rho+2\rho^2(\sin\rho+\cos\rho)+\rho^3(\cos\rho-\sin\rho), \quad (9)$$

$$(P/kT)_{\text{cubes}}=\rho+4\rho^2(\sin\rho+\cos\rho)+5\rho^3(\cos\rho-\sin\rho) -\rho^4(\sin\rho+\cos\rho). \quad (10)$$

Equations (8)–(10) are readily checked by expanding $\sin\rho$ and $\cos\rho$ in Maclaurin's series. The *complete graph* equations of state are plotted in Fig. 1. We see that the contribution of *complete graphs* to the pressure is monotone increasing with density in one and two dimensions, and has a maximum in the hard cubes case for a volume about 4/3 the closest-packed volume.

In Appendix II we show that the value of a *star* integral of $\binom{n}{2}-1$ *lines* is $(-)^{1+[n/2]}\{n+(2/[n-1])\}^d$. Noting that such a *star* may be labeled in $\binom{n}{2}$ ways one can calculate the additional contribution of all such *stars* to the pressure for lines, squares, and cubes. Adding these contributions to (8)–(10) we find

$$(P/kT)_{\text{lines}}=\rho+2\rho^2+4\rho^3+(\tfrac{1}{2}\rho^4+2\rho^3-\rho^2)\sin\rho +(\tfrac{1}{2}\rho^4-2\rho^3-\rho^2)\cos\rho, \quad (11)$$

$$(P/kT)_{\text{squares}} =-\rho+8\rho^2+16\rho^3+(-\tfrac{1}{2}\rho^5+4\rho^4+8\rho^3-4\rho^2-2\rho)\sin\rho +(\tfrac{1}{2}\rho^5+4\rho^4-8\rho^3-4\rho^2+2\rho)\cos\rho, \quad (12)$$

$$(P/kT)_{\text{cubes}} =-5\rho+\{\text{Ci}(\rho)-\text{Si}(\rho)-\gamma-\ln\rho\}(4\rho)+32\rho^2+64\rho^3 +(-\tfrac{1}{2}\rho^6-6\tfrac{1}{2}\rho^5+25\rho^4+33\rho^3-18\rho^2-6\rho)\sin\rho +(-\tfrac{1}{2}\rho^6+6\tfrac{1}{2}\rho^5+25\rho^4-33\rho^3-18\rho^2+6\rho)\cos\rho. \quad (13)$$

In (13) Ci and Si are the cosine and sine integrals and γ is the Euler-Mascheroni constant. The equations of state given by (11)–(13) are plotted in Fig. 2. The pressure in the dense gas region is increased by orders of magnitude over the *complete graph* contribution. It is therefore unlikely that the (tedious) extension of this method to *graphs* of $n-2$, $n-3$, ⋯ *lines* would yield an equation of state more reliable than the available seven-term virial expansion. We have gone no further in this direction.

3. RADIAL DISTRIBUTION FUNCTION FROM THREE APPROXIMATE INTEGRAL EQUATIONS

Percus and Yevick,[7] using collective coordinates, have derived an approximate integral equation for the radial distribution function in terms of the intermo-

[21] In the remainder of this section, and throughout Appendix II, $[n/2]$ is used to indicate $n/2$ for n even, and $(n-1)/2$ for n odd.

lecular potential. Broyles[22] has applied the Percus–Yevick equation to the Lennard–Jones potential, obtaining reasonable agreement with the earlier Monte Carlo[23] calculations. The Kirkwood[8] and convolution[9] integral equations are based respectively on the superposition approximation for the triplet distribution function, and the neglect of all *elementary graphs* in an exact integral equation for the pair distribution function. The results of the Kirkwood equation calculations for hard spheres[24] and modified Lennard-Jones molecules[25] indicate that considerable discrepancies between experimental (Monte Carlo,[26] molecular dynamics,[27] and argon[28]) and calculated radial distribution functions exist in the dense gas region. The Kirkwood equation does predict the observed[26,27] hard-sphere phase transition. Some numerical results for the convolution equation as applied to hard sphere and

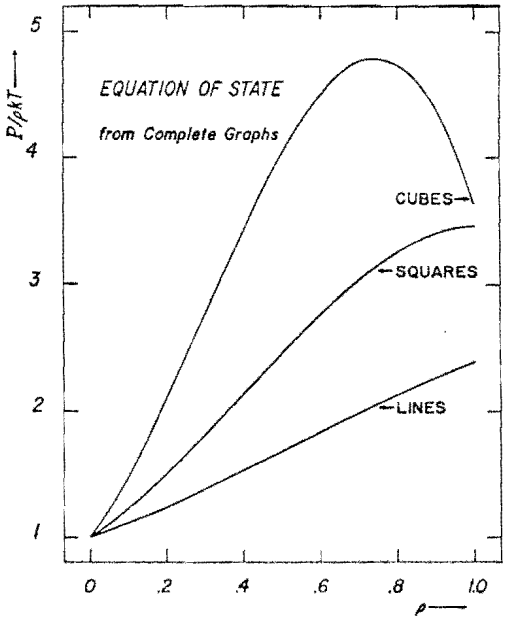

FIG. 1. Equation of state for hard lines, squares, and cubes, using *complete graphs* only. ρ is the ratio of the closest-packed volume to the total volume.

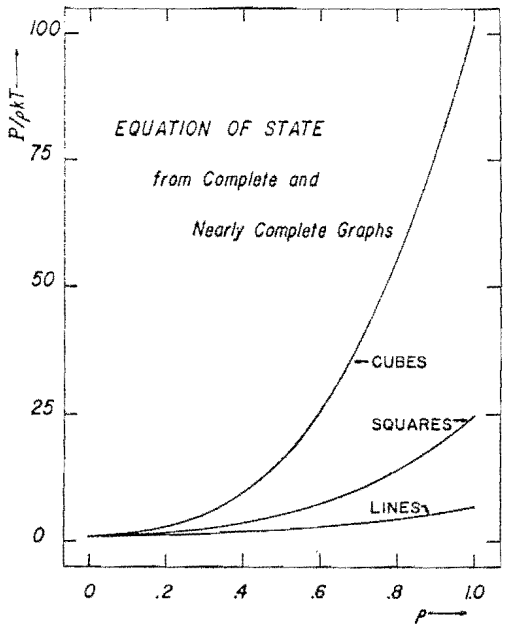

FIG. 2. Equation of state for hard lines, squares, and cubes, using both *complete* and *nearly complete graphs*. ρ is the ratio of the closest-packed volume to the total volume.

Lennard-Jones molecules have been presented by Klein.[29]

In this section we calculate the first four terms of the number density expansion of the radial distribution function for the three integral equations mentioned above; comparisons of this kind have been made for hard sphere[30] and "Gaussian"[31] molecules. The integral equations with which we deal are

$$\exp[\phi(\mathbf{r})/kT]g(\mathbf{r}) = 1+\rho\int f_{23}\exp(\phi_{23}/kT)g_{23}$$
$$\times[f_{13}\exp(\phi_{13}/kT)g_{13}+\exp(\phi_{13}/kT)g_{13}-1]d\mathbf{r}_3, \quad \text{(PY)}$$

$$\ln\{\exp[\lambda\phi(\mathbf{r})/kT]g(\mathbf{r},\lambda)\}$$
$$=\rho\int_0^\lambda d\lambda\int[-g_{13}(\lambda)\phi_{13}/kT](g_{23}-1)d\mathbf{r}_3, \quad \text{(K)}$$

$$\ln\{\exp[\phi(\mathbf{r})/kT]g(\mathbf{r})\}$$
$$=\rho\int[g_{13}-1-\ln g_{13}-(\phi_{13}/kT)](g_{23}-1)d\mathbf{r}_3. \quad \text{(C)}$$

[22] A. A. Broyles, J. Chem. Phys. **34**, 1068 (1961); **35**, 493 (1961). Broyles has also made similar calculations using the Born-Green-Yvon integral equation: J. Chem. Phys. **33**, 456 (1960); **34**, 359 (1961).

[23] W. W. Wood and F. R. Parker, J. Chem. Phys. **27**, 720 (1957).

[24] J. G. Kirkwood and E. M. Boggs, J. Chem. Phys. **10**, 394 (1942).

[25] J. G. Kirkwood, V. A. Lewinson, and B. J. Alder, J. Chem. Phys. **20**, 929 (1952).

[26] W. W. Wood, F. R. Parker, and J. D. Jacobson, Nuovo cimento, Suppl. Vol. **9**, 133 (1958).

[27] B. J. Alder and T. E. Wainwright, *Proceedings of the International Symposium on Transport Processes in Statistical Mechanics, Brussels, 1956*, edited by I. Prigogine (Interscience Publishers, Inc., New York, 1958), p. 97.

[28] A. Eisenstein and N. S. Gingrich, Phys. Rev. **62**, 261 (1942); N. S. Gingrich and C. W. Tompson, J. Chem. Phys. **36**, 2398 (1962).

[29] M. Klein, dissertation, University of Maryland, 1962; this is an excellent description of the calculation and interpretation of radial distribution functions from the convolution integral equation; some of the numerical results referred to above were presented by Klein at the March meeting of the American Physical Society, Baltimore, 1962.

[30] B. R. A. Nijboer and L. Van Hove, Phys. Rev. **85**, 777 (1952); G. Stell, J. Chem. Phys. **36**, 1817 (1962) and references given in the latter paper.

[31] See G. E. Uhlenbeck and G. W. Ford, *Studies in Statistical Mechanics*, edited by J. de Boer and G. E. Uhlenbeck (Interscience Publishers, Inc., New York, 1962), Vol. I, p. 194; E. Helfand presented preliminary results of a calculation of $g_1(r)\cdots g_5(r)$ for "Gaussian" molecules at the March meeting of the American Physical Society, Baltimore, 1962.

Each of these equations may be solved [as a series expansion of $\exp[\phi(\mathbf{r})/kT]g(\mathbf{r})\equiv\mathcal{G}(\mathbf{r})$ in the number density] by the standard Liouville–Neumann method[32]; equivalently one can substitute a power series for $\mathcal{G}(\mathbf{r})$ or for $\Psi(\mathbf{r})\equiv -kT\ln g(\mathbf{r})$ into the equations, equate like powers of ρ, and thus obtain solutions. Using

$$g(\mathbf{r})\equiv\exp\{-\phi(\mathbf{r})/kT\}\times\{\exp[\alpha(\mathbf{r})\rho+\beta(\mathbf{r})\rho^2+\gamma(\mathbf{r})\rho^3+\cdots]\}=\exp\{-\Psi(\mathbf{r})/kT\}, \quad (14)$$

[where $\alpha(\mathbf{r})$, $\beta(\mathbf{r})$, and $\gamma(\mathbf{r})$ depend in the Kirkwood case upon λ as well as $\mathbf{r}$] we introduce f functions and expand the exponential in brackets in (14) to get explicit expressions for $\alpha(\mathbf{r})$, $\beta(\mathbf{r})$, and $\gamma(\mathbf{r})$ in terms of *doubly rooted graph* integrals. We had intended to treat the Born-Green-Yvon equation[10] in this way too, but found that for squares and cubes there are no solutions of the form (14) which are symmetric in x, y, and z.

As an illustration of the Liouville-Neumann method we apply (14) to the Kirkwood integral equation [replacing $\phi(\mathbf{r})$ by $\lambda\phi(\mathbf{r})$ in (14)]. The Percus–Yevick and convolution equations are solved in the same way, but without the complication of the coupling parameter λ. We substitute (14) into (K), expand the exponential, and equate coefficients of like powers of ρ to obtain the following equations for $\alpha(\mathbf{r},\lambda)$, $\beta(\mathbf{r},\lambda)$, and $\gamma(\mathbf{r},\lambda)$:

$$\alpha(\mathbf{r},\lambda)=\int_0^\lambda d\lambda\int(-\phi_{13}/kT)\,\exp\,(-\lambda\phi_{13}/kT)f_{23}d\mathbf{r}_3, \quad (15)$$

$$\beta(\mathbf{r},\lambda)=\int_0^\lambda d\lambda\int(-\phi_{13}/kT)\,\exp(-\lambda\phi_{13}/kT)[\alpha_{13}(\lambda)f_{23}+f_{23}\alpha_{23}+\alpha_{23}]d\mathbf{r}_3, \quad (16)$$

$$\gamma(\mathbf{r},\lambda)=\int_0^\lambda d\lambda\int(-\phi_{13}/kT)\,\exp(-\lambda\phi_{13}/kT)[\tfrac{1}{2}\alpha_{13}^2(\lambda)f_{23}+\beta_{13}(\lambda)f_{23}+\alpha_{13}(\lambda)f_{23}\alpha_{23}+\alpha_{13}(\lambda)\alpha_{23}+\tfrac{1}{2}f_{23}\alpha_{23}^2+\tfrac{1}{2}\alpha_{23}^2+f_{23}\beta_{23}+\beta_{23}]d\mathbf{r}_3. \quad (17)$$

We can integrate over λ in (15) to get an explicit equation for $\alpha(\mathbf{r},\lambda)$:

$$\alpha(\mathbf{r},\lambda)=\int f_{13}(\lambda)f_{23}d\mathbf{r}_3=\int \text{⟍}\,d\mathbf{r}_3. \quad (18)$$

Making use of (18) and the definition $\exp(-\lambda\phi_{14}/kT)\equiv f_{14}(\lambda)+1$, [indicating $f(\lambda)$ by a *cross-hatched line* in (18) and (20)] we integrate over λ in (16) and find that $\beta(\mathbf{r},\lambda)$ is given by

$$\beta(\mathbf{r},\lambda)=\int\left\{\left[\frac{\phi_{13}}{\phi_{13}+\phi_{14}}\right][f_{13}(\lambda)f_{14}(\lambda)f_{23}f_{34}+f_{13}(\lambda)f_{23}f_{34}+f_{14}(\lambda)f_{23}f_{34}]-f_{13}(\lambda)f_{23}f_{34}+f_{13}(\lambda)f_{23}f_{24}f_{34}+f_{13}(\lambda)f_{24}f_{34}\right\}d\mathbf{r}_3d\mathbf{r}_4. \quad (19)$$

In general, one cannot reduce the integrand in (19) to a set of the usual *doubly rooted graphs* (with *lines* indicating f functions only). For hard lines, squares, and cubes (as well as spheres) however, we see that the fraction $\phi_{13}/(\phi_{13}+\phi_{14})$ may take on the values 0, $\frac{1}{2}$, or 1 only, and we may indicate the value of this fraction by adding appropriate f functions to the integrand of (19). For example, the term

$$\int\left[\frac{\phi_{13}}{\phi_{13}+\phi_{14}}\right]f_{13}(\lambda)f_{23}f_{34}d\mathbf{r}_3d\mathbf{r}_4$$

may be replaced by

$$\int[f_{13}(\lambda)f_{23}f_{34}+\tfrac{1}{2}f_{13}(\lambda)f_{14}f_{23}f_{34}]d\mathbf{r}_3d\mathbf{r}_4,$$

[32] H. Margenau and G. M. Murphy, *The Mathematics of Physics and Chemistry* (D. Van Nostrand Company, Inc., Princeton, New Jersey, 1943), p. 504.

so that we have $\int f_{13}(\lambda) f_{23} f_{34} d\mathbf{r}_3 d\mathbf{r}_4$ if molecules 1 and 4 do not overlap, and $\frac{1}{2}\int f_{13}(\lambda) f_{23} f_{34} d\mathbf{r}_3 d\mathbf{r}_4$ if they do. Proceeding in this way we get the following expression for $\beta(\mathbf{r}, \lambda)$:

$$\beta(\mathbf{r}, \lambda) = \tfrac{1}{2}\int [\,\text{ 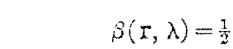 }\,] d\mathbf{r}_3 d\mathbf{r}_4, \tag{20}$$

where we are using the position convention $\begin{smallmatrix} 3 & 4 \\ 1 & 2 \end{smallmatrix}$. In the same straightforward way one can use (18) and (20) to convert (17) into an explicit equation for $\gamma(\mathbf{r}, \lambda)$ in terms of *doubly rooted graphs*. The fraction $\phi_{13}/(\phi_{13}+\phi_{14}+\phi_{15})$ is treated by a simple extension of our arguments regarding the simpler case $\phi_{13}/(\phi_{13}+\phi_{14})$. Passing to the limit, $\lambda \to 1$, we obtain $\alpha(\mathbf{r})$, $\beta(\mathbf{r})$, and $\gamma(\mathbf{r})$ for the fully coupled system of interest

$$\alpha(\mathbf{r}) = \int \wedge\, d\mathbf{r}_3, \tag{21}$$

$$\beta(\mathbf{r}) = \tfrac{1}{2}\int [\,\text{ 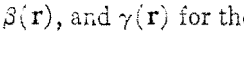 }\,] d\mathbf{r}_3 d\mathbf{r}_4, \tag{22}$$

$$\gamma(\mathbf{r}) = \tfrac{1}{6}\int [\,\text{}\,] d\mathbf{r}_3 d\mathbf{r}_4 d\mathbf{r}_5. \tag{23}$$

We can then find $\mathcal{G}(\mathbf{r})$ through terms in ρ^3 for the Kirkwood equation by introducing (21)–(23) into (14) and expanding the exponential. The Percus–Yevick and convolution equations require considerably less manipulation. In (24) we give the results.[33] The four numbers preceding each type of *doubly rooted graph* in (24) indicate the number of times that this graph type occurs in the Percus–Yevick, Kirkwood, convolution, and exact expressions, respectively. The exact result is included for comparison.

$\mathcal{G}(\mathbf{r})$ (PY, K, C, E) =

$$1+\rho\int (1,1,1,1) \wedge d\mathbf{r}_3 + \tfrac{1}{2}\rho^2 \int [\,(0,1,1,1)\,\text{ 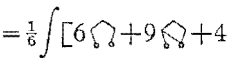 } + (2,2,2,2)\,\text{} + (4,3,4,4)\,\text{} + (0,0,0,1)\,\text{}\,] d\mathbf{r}_3 d\mathbf{r}_4$$

$$+\tfrac{1}{6}\rho^3 \int [\,(0,1,1,1)\,\text{ 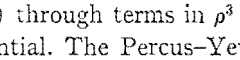 } + (0,6,6,6)\,\text{} + (0,9,12,12)\,\text{} + (0,0,0,3)\,\text{} + (6,6,6,6)\,\text{} + (12,9,12,12)\,\text{}$$

$$+(6,4,6,6)\,\text{ 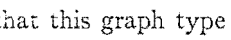 } + (12,8,12,12)\,\text{} + (0,3,6,6)\,\text{} + (0,0,0,3)\,\text{} + (12,9,12,12)\,\text{} + (12,4,12,12)\,\text{}$$

$$+(0,0,0,12)\,\text{} + (0,4,6,6)\,\text{} + (6,3,6,6)\,\text{} + (0,0,0,6)\,\text{} + (0,0,0,12)\,\text{} + (0,0,0,6)\,\text{}$$

$$+(0,0,0,3)\,\text{ 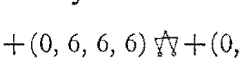 } + (0,0,0,6)\,\text{} + (0,0,0,6)\,\text{} + (0,0,0,3)\,\text{} + (0,0,0,6)\,\text{} + (0,0,0,1)\,\text{}\,] d\mathbf{r}_3 d\mathbf{r}_4 d\mathbf{r}_5. \tag{24}$$

We note that in (24) $\mathcal{G}(\mathbf{r})$ (PY) contains no *composite graphs*, and that none of the three integral equations produces *elementary graphs*. These facts have been shown in general for the Percus–Yevick[7] and convolution[9] equations. We stress again that $\mathcal{G}(\mathbf{r})$ (K) is obtained in this relatively simple form because $\phi(\mathbf{r})$ takes on the values of zero and infinity only.

As has previously been pointed out, $\mathcal{G}(\mathbf{r})$ is a symmetric function of x, y, and z for cubes; each *graph* in (24) contributes a term of the form

$$P_i(|x|) P_i(|y|) P_i(|z|),$$

where P_i is a polynomial obtained by integrating over the ith *doubly rooted* one-dimensional *graph*.[5] In order to make a visual comparison of different distribution functions it is convenient to have "radial" distribution functions of one space coordinate only. The natural distribution function to pick is Cartesian, obtained by averaging the two-dimensional $\mathcal{G}(x, y)$ around the perimeter of a square of side length $2r$ and the three-dimensional $\mathcal{G}(x, y, z)$ over the surface of a cube of side length $2r$. We denote the result of this averaging procedure by $\mathcal{G}(r) \equiv \sum g_n(r) \rho^n$. To illustrate the averaging process we consider the three-dimensional

[33] Most of these results are not new. In particular Percus and Yevick[7] show which *graphs* contribute to $g(r)$ (PY). Stell[30] has recently made a calculation (independently) of $g_1(r)$ and $g_2(r)$ from the Kirkwood equation. Those *graphs* contributing to the convolution equation $g(r)$ are obvious from the structure of the equation's derivation [G. S. Rushbrooke and P. Hutchinson, Physica **27**, 647 (1961)].

TABLE V. $\mathcal{G}(r)$ for hard lines of unit length. E, PY, K, and C indicate exact, Percus–Yevick, Kirkwood, and convolution results, respectively.

E	$(0<r<1)$	$:1+\rho(2-r)+(\rho^2/4)($	$14-12r+2r^2)+(\rho^3/36)($	$204-234r+72r^2-6r^3)$
E	$(1<r<2)$	$:1+\rho(2-r)+(\rho^2/4)($	$14-12r+2r^2)+(\rho^3/36)($	$204-234r+72r^2-6r^3)$
E	$(2<r<3)$	$:1+(\rho^2/4)(-18+12r-2r^2)+(\rho^3/36)(-588+522r-144r^2+12r^3)$		
E	$(3<r<4)$	$:1+(\rho^3/36)($	$384-288r+72r^2-6r^3)$	
PY	$(0<r<1)$	$:1+\rho(2-r)+(\rho^2/4)($	$12-8r)+(\rho^3/36)($	$144-108r)$
PY	$(1<r<2)$	$:1+\rho(2-r)+(\rho^2/4)($	$14-12r+2r^2)+(\rho^3/36)($	$204-234r+72r^2-6r^3)$
PY	$(2<r<3)$	$:1+(\rho^2/4)(-18+12r-2r^2)+(\rho^3/36)(-588+522r-144r^2+12r^3)$		
PY	$(3<r<4)$	$:1+(\rho^3/36)($	$384-288r+72r^2-6r^3)$	
K	$(0<r<1)$	$:1+\rho(2-r)+(\rho^2/4)($	$14-14r+3r^2)+(\rho^3/36)($	$200-285r+132r^2-25r^3)$
K	$(1<r<2)$	$:1+\rho(2-r)+(\rho^2/4)($	$14-14r+3r^2)+(\rho^3/36)($	$224-327r+144r^2-19r^3)$
K	$(2<r<3)$	$:1+(\rho^2/4)(-18+12r-2r^2)+(\rho^3/36)(-426+414r-126r^2+12r^3)$		
K	$(3<r<4)$	$:1+(\rho^3/36)($	$384-288r+72r^2-6r^3)$	
C	$(0<r<1)$	$:1+\rho(2-r)+(\rho^2/4)($	$20-16r+2r^2)+(\rho^3/36)($	$408-468r+144r^2-18r^3)$
C	$(1<r<2)$	$:1+\rho(2-r)+(\rho^2/4)($	$22-20r+4r^2)+(\rho^3/36)($	$492-648r+252r^2-30r^3)$
C	$(2<r<3)$	$:1+(\rho^2/4)(-18+12r-2r^2)+(\rho^3/36)(-912+846r-252r^2+24r^3)$		
C	$(3<r<4)$	$:1+(\rho^3/36)($	$384-288r+72r^2-6r^3)$	

integral $\mathcal{G}(\mathbf{r})\equiv\int\!\!\int\!\!\int d\mathbf{r}_3$. The value of this integral is $(2-|x|)(2-|y|)(2-|z|)$ for $-2<x,\ y,\ z<2$, and zero otherwise. By symmetry we see that the average value of $\mathcal{G}(x,\ y,\ z)$ on the surface of a cube of side length $2r$ is identical with the average over the region $(0<x,\ y<r,\ z\equiv r)$. The area of this region is r^2, and accordingly $\mathcal{G}(r)$ is given by

$$\mathcal{G}(r)=\frac{2-r}{r^2}\int_0^r\int_0^r(2-x)(2-y)\,dxdy \qquad (0<r<2),$$

$$\mathcal{G}(r)=0 \qquad (2<r). \tag{25}$$

Because the values of the integrals in (24) have been tabulated[5] as functions of x, and are therefore known as functions of x, y in the two-dimensional case, and x, y, z in the three-dimensional case, we can average these integrals as in (25). Then, in one, two, and three dimensions, the quantities[34] $g_1(r)$, $g_2(r)$, and $g_3(r)$ can be calculated for each of the approximate integral equations, as well as for the exact case. The analytical expressions for all of these functions are given in Tables V–VII; $\exp[-\phi(r)/kT]g_2(r)$ and $\exp[-\phi(r)/kT]g_3(r)$ are plotted in Figs. 3–8. We see that the Percus-Yevick equation is (to the order of the terms retained) exact in one dimension and gives the most faithful rendering of the two and three-dimensional $\exp[-\phi(r)/kT]g_n(r)$ as well. As the density of a gas increases from zero, the ρ^2 and higher order terms become increasingly more important in their contribution to the Cartesian distribution function $\mathcal{G}(r)$. Accordingly, for these molecules at least, in the density region where the terms we have calculated provide an adequate description of $\mathcal{G}(r)$, the Percus–Yevick distribution function is the most reliable of the three approximations. One also sees that the Kirkwood results are more smooth and the convolution results less smooth than the exact curves. The discrepancies between the exact and approximate curves increase with the dimensionality of the molecules. Although the Percus–Yevick curves are more "accurate" than those derived from the Kirkwood or convolution equations, the question of the relative reliability of thermodynamic information derived from these approximate distribution functions is more difficult; we discuss it in the following sections.

[34] The $g_n(\mathbf{r})$ are defined by (2) and (4).

4. VIRIAL COEFFICIENTS FROM THE PERCUS-YEVICK, KIRKWOOD, AND CONVOLUTION EQUATIONS

The pressure of a gas can be determined from $g(\mathbf{r})$ or $\mathcal{G}(r)$ by means of (i) the Ornstein–Zernicke relation,[16]

$$kT(\partial\rho/\partial P)_{N,T}=1+\rho\int[g(\mathbf{r})-1]d\mathbf{r}, \tag{26}$$

or (ii) the virial theorem,[17] which latter leads to

$$\frac{P}{kT}=\rho-\frac{\rho^2}{2dkT}\int g(\mathbf{r})[\mathbf{r}\cdot\nabla\phi(\mathbf{r})]d\mathbf{r}. \tag{27}$$

TABLE VI. $\mathcal{G}(r)$ for hard squares of unit area. E, PY, K, and C indicate exact, Percus-Yevick, Kirkwood, and convolution results, respectively.

$$E(0<r<1):1+(\rho/2)(8-6r+r^2)+(\rho^2/24)(300-396r+160r^2-20r^3)$$
$$+(\rho^3/864)(28\,992-52\,704r+32\,760r^2-7920r^3+324r^4+168r^5-12r^6)$$

$$E(1<r<2):1+(\rho/2)(8-6r+r^2)+(\rho^2/24)(6r^{-1}+278-376r+164r^2-30r^3+2r^4)$$
$$+(\rho^3/864)(1476r^{-1}+23\,082-46\,152r+32\,502r^2-11\,100r^3+1962r^4-168r^5+6r^6)$$

$$E(2<r<3):1+(\rho^2/24)(54r^{-1}-522+492r-180r^2+30r^3-2r^4)$$
$$+(\rho^3/864)(13\,980r^{-1}-124\,482+155\,232r-83\,118r^2+23\,820r^3-3870r^4+336r^5-12r^6)$$

$$E(3<r<4):1+(\rho^3/864)(-24\,576r^{-1}+116\,736-115\,200r+52\,608r^2-13\,440r^3+2016r^4-168r^5+6r^6)$$

$$PY(0<r<1):1+(\rho/2)(8-6r+r^2)+(\rho^2/24)(216-216r+24r^2+20r^3-4r^4)$$
$$+(\rho^3/864)(13\,056-14\,688r+864r^2+2760r^3-684r^4+12r^6)$$

$$PY(1<r<2):1+(\rho/2)(8-6r+r^2)+(\rho^2/24)(-10r^{-1}+294-380r+164r^2-30r^3+2r^4)$$
$$+(\rho^3/864)(-2916r^{-1}+33\,054-56\,952r+40\,062r^2-14\,580r^3+2970r^4-336r^5+18r^6)$$

$$PY(2<r<3):1+(\rho^2/24)(54r^{-1}-522+492r-180r^2+30r^3-2r^4)$$
$$+(\rho^3/864)(19\,164r^{-1}-129\,666+156\,960r-83\,310r^2+23\,820r^3-3870r^4+336r^5-12r^6)$$

$$PY(3<r<4):1+(\rho^3/864)(-24\,576r^{-1}+116\,736-115\,200r+52\,608r^2-13\,440r^3+2016r^4-168r^5+6r^6)$$

$$K(0<r<1):1+(\rho/2)(8-6r+r^2)+(\rho^2/24)(300-450r+202r^2-25r^3-r^4)$$
$$+(\rho^3/864)(28\,160-61\,704r+48\,938r^2-16\,040r^3+897r^4+602r^5-73r^6)$$

$$K(1<r<2):1+(\rho/2)(8-6r+r^2)+(\rho^2/24)(6r^{-1}+282-450r+238r^2-55r^3+5r^4)$$
$$+(\rho^3/864)(-640r^{-1}+34\,646-80\,640r+75\,242r^2-36\,290r^3+9801r^4-1428r^5+89r^6)$$

$$K(2<r<3):1+(\rho^2/24)(54r^{-1}-522+492r-180r^2+30r^3-2r^4)$$
$$+(\rho^3/864)(10\,092r^{-1}-88\,032+120\,564r-71\,256r^2+22\,740r^3-4176r^4+420r^5-18r^6)$$

$$K(3<r<4):1+(\rho^3/864)(-24\,576r^{-1}+116\,736-115\,200r+52\,608r^2-13\,440r^3+2016r^4-168r^5+6r^6)$$

$$C(0<r<1):1+(\rho/2)(8-6r+r^2)+(\rho^2/24)(408-504r+184r^2-20r^3)$$
$$+(\rho^3/864)(53\,376-95\,904r+57\,792r^2-12\,600r^3-756r^4+672r^5-36r^6)$$

$$C(1<r<2):1+(\rho/2)(8-6r+r^2)+(\rho^2/24)(-10r^{-1}+486-668r+324r^2-70r^3+6r^4)$$
$$+(\rho^3/864)(-3144r^{-1}+79\,284-159\,480r+129\,624r^2-55\,680r^3+13\,680r^4-1848r^5+108r^6)$$

$$C(2<r<3):1+(\rho^2/24)(54r^{-1}-522+492r-180r^2+30r^3-2r^4)$$
$$+(\rho^3/864)(30\,180r^{-1}-210\,666+265\,608r-149\,814r^2+46\,500r^3-8406r^4+840r^5-36r^6)$$

$$C(3<r<4):1+(\rho^3/864)(-24\,576r^{-1}+116\,736-115\,200r+52\,608r^2-13\,440r^3+2016r^4-168r^5+6r^6)$$

Differentiating $\exp[-\phi(\mathbf{r})/kT]$ gives $\nabla\phi(\mathbf{r})=-kT\exp[\phi(\mathbf{r})/kT]\tilde{\mathfrak{o}}_s$, where $\tilde{\mathfrak{o}}_s$ is a delta function which is nonzero only on the surface of a d-dimensional cube of twice the molecular side length, in complete analogy with the usual treatment for spheres.[35] Using this technique (27) assumes the particularly simple form

$$P/kT=\rho+\rho^2B_2\mathcal{G}(1)=\rho+\rho^2B_2g(1), \qquad (28)$$

for hard lines, squares, and cubes ($\sigma\equiv1$). We may therefore obtain the virial expansion of the pressure from either (26) or (28), using [in (26)] $2dr$, $8rdr$, and $24r^2dr$ for the one-, two-, and three-dimensional $d\mathbf{r}$'s, and $g(r)$ for $g(\mathbf{r})$. As an example let us calculate B_4 for squares according to the Kirkwood equation.

Inverting the Ornstein-Zernicke relation (26) gives

$$(1/kT)(\partial P/\partial\rho)_{N,T}=[1+\rho F(\rho)]^{-1}$$
$$\equiv1-\rho F+\rho^2F^2-\rho^3F^3+\cdots, \qquad (29)$$

[35] T. L. Hill, *Statistical Mechanics* (McGraw-Hill Book Company, Inc., New York, 1956), p. 214.

TABLE VII. $g(r)$ for hard cubes of unit volume. E, PY, K, and C indicate exact, Percus–Yevick, Kirkwood, and convolution results, respectively.

E $(0<r<1)$:
$1+(\rho/4)(32-32r+10r^2-r^3)+(\rho^2/144)(6552-11\,808r+7680r^2-2520r^3+644r^4-160r^5+20r^6)$
$+(\rho^3/20\,736)(4\,322\,304-11\,003\,904r+10\,748\,160r^2-5\,520\,096r^3+1\,918\,560r^4-590\,784r^5$
$+183\,528r^6-50\,340r^7+10\,032r^8-1080r^9)$

E $(1<r<2)$:
$1+(\rho/4)(32-32r+10r^2-r^3)+(\rho^2/144)(-66r^{-2}+656r^{-1}+4688-9808r+6980r^2-2472r^3+476r^4-48r^5+2r^6)$
$+(\rho^3/20\,736)(-125\,940r^{-2}+1\,325\,502r^{-1}-53\,400-4\,531\,590r+5\,628\,840r^2-2\,663\,748r^3+296\,352r^4+237\,780r^5$
$-120\,780r^6+26\,130r^7-2904r^8+138r^9)$

E $(2<r<3)$:
$1+(\rho^2/144)(-162r^{-2}+3024r^{-1}-16\,056+18\,576r-9900r^2+2928r^3-504r^4+48r^5-2r^6)$
$+(\rho^3/20\,736)(40\,020r^{-2}+4\,098\,426r^{-1}-26\,285\,736+41\,189\,706r-31\,510\,440r^2+14\,421\,492r^3-4\,304\,160r^4+866\,148r^5$
$-117\,324r^6+10\,290r^7-528r^8+12r^9)$

E $(3<r<4)$:
$1+(\rho^3/20\,736)(1\,572\,864r^{-2}-13\,762\,560r^{-1}+39\,616\,512-44\,457\,984r+27\,279\,360r^2-10\,579\,968r^3+2\,774\,016r^4$
$-504\,576r^5+63\,360r^6-5280r^7+264r^8-6r^9)$

PY $(0<r<1)$:
$1+(\rho/4)(32-32r+10r^2-r^3)+(\rho^2/144)(3888-5184r+1080r^2+792r^3-252r^4-32r^5+12r^6)$
$+(\rho^3/20\,736)(1\,069\,056-1\,603\,584r+103\,680r^2+636\,768r^3-161\,280r^4-68\,352r^5$
$+27\,432r^6+180r^7-1056r^8+108r^9)$

PY $(1<r<2)$:
$1+(\rho/4)(32-32r+10r^2-r^3)+(\rho^2/144)(-34r^{-2}-144r^{-1}+5848-10\,448r+7140r^2-2488r^3+476r^4-48r^5+2r^6)$
$+(\rho^3/20\,736)(42\,228r^{-2}-1\,000\,182r^{-1}+6\,415\,728-13\,523\,034r+13\,569\,000r^2-7\,525\,764r^3+2\,424\,912r^4-429\,228r^5$
$+25\,452r^6+4830r^7-1056r^8+66r^9)$

PY $(2<r<3)$:
$1+(\rho^2/144)(-162r^{-2}+3024r^{-1}-16\,056+18\,576r-9900r^2+2928r^3-504r^4+48r^5-2r^6)$
$+(\rho^3/20\,736)(-395\,436r^{-2}+6\,773\,370r^{-1}-29\,790\,120+43\,320\,906r-32\,236\,200r^2+14\,566\,644r^3-4\,320\,288r^4+866\,916r^5$
$-117\,324r^6+10\,290r^7-528r^8+12r^9)$

PY $(3<r<4)$:
$1+(\rho^3/20\,736)(1\,572\,864r^{-2}-13\,762\,560r^{-1}+39\,616\,512-44\,457\,984r+27\,279\,360r^2-10\,579\,968r^3+2\,774\,016r^4$
$-504\,576r^5+63\,360r^6-5280r^7+264r^8-6r^9)$

K $(0<r<1)$:
$1+(\rho/4)(32-32r+10r^2-r^3)+(\rho^2/144)(6552-13\,104r+9030r^2-2862r^3+623r^4-152r^5+21r^6)$
$+(\rho^3/20\,736)(4\,192\,256-12\,476\,928r+14\,397\,040r^2-8\,292\,948r^3+2\,680\,664r^4-613\,144r^5$
$+186\,252r^6-63\,145r^7+12\,958r^8-1213r^9)$

K $(1<r<2)$:
$1+(\rho/4)(32-32r+10r^2-r^3)+(\rho^2/144)(-66r^{-2}+648r^{-1}+4980-12\,408r+10\,560r^2-4590r^3+1127r^4-152r^5+9r^6)$
$+(\rho^3/20\,736)(-28\,468r^{-2}+140\,158r^{-1}+4\,861\,544-16\,959\,238r+23\,753\,600r^2-18\,132\,432r^3+8\,552\,712r^4-2\,644\,136r^5$
$+545\,994r^6-73\,665r^7+5940r^8-217r^9)$

K $(2<r<3)$:
$1+(\rho^2/144)(-162r^{-2}+3024r^{-1}-16\,056+18\,576r-9900r^2+2928r^3-504r^4+48r^5-2r^6)$
$+(\rho^3/20\,736)(73\,392r^{-2}+2\,494\,788r^{-1}-17\,844\,456+31\,432\,020r-26\,815\,680r^2+13\,686\,984r^3-4\,585\,392r^4+1\,048\,200r^5$
$-164\,016r^6+16\,980r^7-1056r^8+30r^9)$

K $(3<r<4)$:
$1+(\rho^3/20\,736)(1\,572\,864r^{-2}-13\,762\,560r^{-1}+39\,616\,512-44\,457\,984r+27\,279\,360r^2-10\,579\,968r^3+2\,774\,016r^4$
$-504\,576r^5+63\,360r^6-5280r^7+264r^8-6r^9)$

C $(0<r<1)$:
$1+(\rho/4)(32-32r+10r^2-r^3)+(\rho^2/144)(8496-14\,400r+8760r^2-2664r^3+644r^4-160r^5+20r^6)$
$+(\rho^3/20\,736)(7\,317\,504-18\,266\,112r+17\,030\,400r^2-7\,855\,776r^3+2\,149\,056r^4-563\,328r^5$
$+219\,672r^6-69\,780r^7+12\,672r^8-1128r^9)$

C $(1<r<2)$:
$1+(\rho/4)(32-32r+10r^2-r^3)+(\rho^2/144)(-34r^{-2}-144r^{-1}+10\,456-19\,664r+14\,820r^2-5944r^3+1372r^4-176r^5+10r^6)$
$+(\rho^3/20\,736)(-42\,816r^{-2}-483\,516r^{-1}+12\,656\,352-34\,846\,464r+41\,979\,360r^2-28\,945\,944r^3+12\,786\,144r^4-3\,807\,408r^5$
$+773\,496r^6-104\,160r^7+8448r^8-312r^9)$

C $(2<r<3)$:
$1+(\rho^2/144)(-162r^{-2}+3024r^{-1}-16\,056+18\,576r-9900r^2+2928r^3-504r^4+48r^5-2r^6)$
$+(\rho^3/20\,736)(-769\,980r^{-2}+11\,906\,826r^{-1}-52\,169\,880+78\,062\,394r-61\,072\,200r^2+29\,571\,732r^3-9\,580\,032r^4+2\,143\,812r^5$
$-331\,164r^6+34\,050r^7-2112r^8+60r^9)$

C $(3<r<4)$:
$1+(\rho^3/20\,736)(1\,572\,864r^{-2}-13\,762\,560r^{-1}+39\,616\,512-44\,457\,984r+27\,279\,360r^2-10\,579\,968r^3+2\,774\,016r^4$
$-504\,576r^5+63\,360r^6-5280r^7+264r^8-6r^9)$

where $F \equiv \int [g(\mathbf{r})-1]d\mathbf{r}$ and the series converges for $|\rho F|<1$. From (24) we calculate F (Kirkwood):

$$F(\mathrm{K}) = \int \text{—} d\mathbf{r}_2 + \int \exp[-\phi(\mathbf{r})/kT]$$

$$\times \left\{ \rho \int \wedge\, d\mathbf{r}_3 + \tfrac{1}{2}\rho^2 \int [2\,\square + \bowtie + 3\,\square] d\mathbf{r}_3 d\mathbf{r}_4 \right\} d\mathbf{r}_2; \tag{30}$$

$$F(\mathrm{K}) = \int \text{—} d\mathbf{r}_2 + \rho \int [\triangle + \wedge] d\mathbf{r}_2 d\mathbf{r}_3$$

$$+ \tfrac{1}{2}\rho^2 \int [3\square + 4\diagdown + 2\sqcap + 3\diagdown] d\mathbf{r}_2 d\mathbf{r}_3 d\mathbf{r}_4. \tag{31}$$

Substituting (31) into (29), integrating with respect to

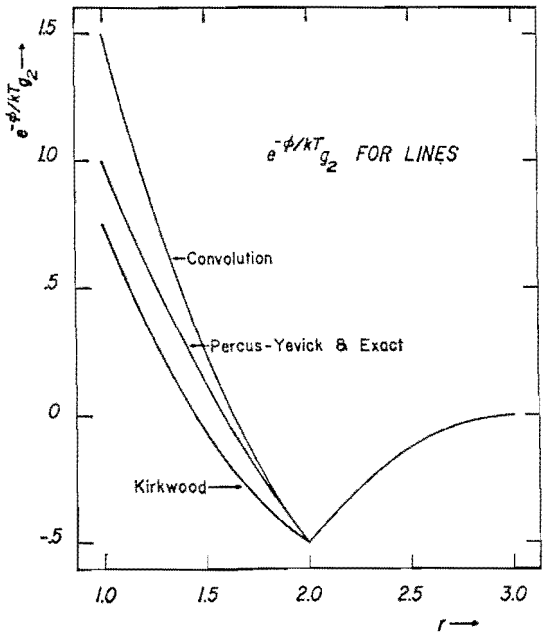

FIG. 3. $\mathrm{Exp}[-\phi(r)/kT]g_2(r)$ for hard lines of unit length according to three integral equations. The exact and Percus-Yevick curves coincide.

ρ (from 0 to ρ), we identify B_4 according to the Ornstein-Zernicke relation as applied to the Kirkwood equation:

$$B_4 = -\tfrac{1}{8}\int [3\square + 4\diagdown - \diagdown] d\mathbf{r}_2 d\mathbf{r}_3 d\mathbf{r}_4. \tag{32}$$

Putting in the appropriate values for the integrals[5] we find in two dimensions $B_4 = -(1/8)[3(16/3)^2 - 4(14/3)^2 - (2)^2(3)^2] = 85/18$.

We can get B_4 according to the virial theorem as applied to the Kirkwood equation (in two dimensions)

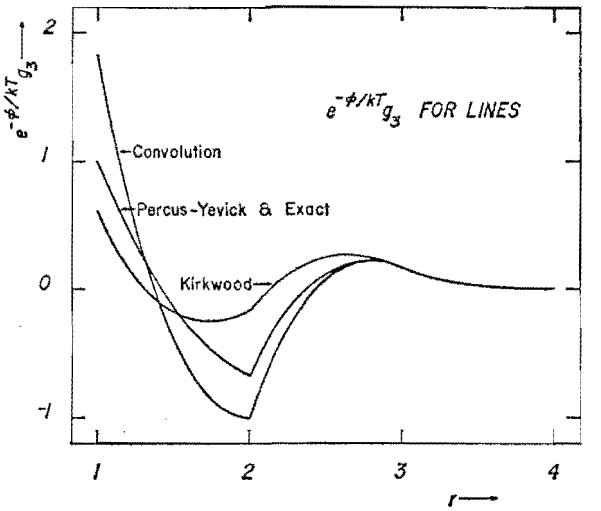

FIG. 4. $\mathrm{Exp}[-\phi(r)/kT]g_3(r)$ for hard lines of unit length according to three integral equations. The exact and Percus-Yevick curves coincide.

by noting that $g_2(1)$ is (from Table VI) 13/12. Thus $B_4 = 2(13/12) = 13/6$.

In the way illustrated above we find the virial coefficients through B_5 for lines, squares, and cubes; B_2 and B_3 are given exactly by all three integral equations from both the Ornstein-Zernicke relation and the virial theorem and so are not tabulated; B_4 and B_5 are displayed in Tables VIII–X. We have also included B_6 from the convolution equation, first getting the *graphs* contributing to $g_4(\mathbf{r})$ by iteration and then substituting these directly into (26) and (28) to gene-

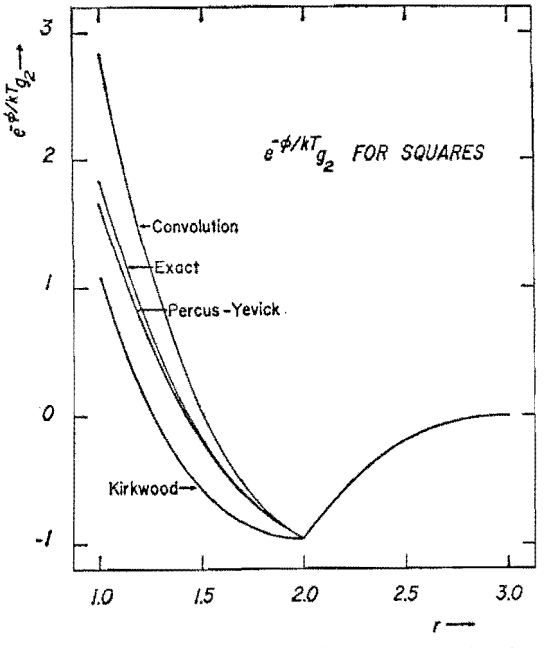

FIG. 5. $\mathrm{Exp}[-\phi(r)/kT]g_2(r)$ for hard squares of unit area according to three integral equations. The exact curve is included for comparison.

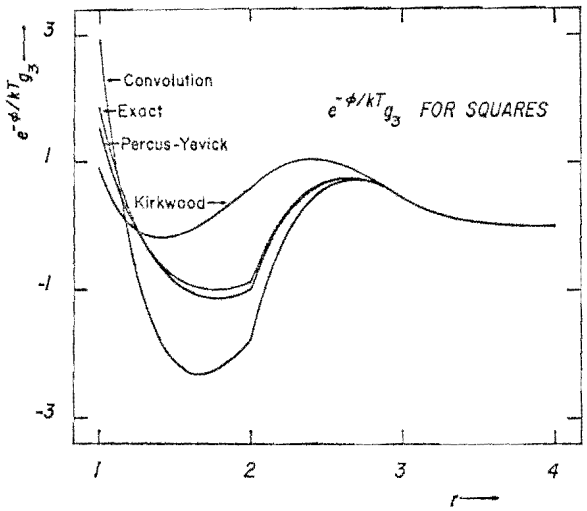

FIG. 6. $\mathrm{Exp}[-\phi(r)/kT]g_3(r)$ for hard squares of unit area according to three integral equations. The exact curve is included for comparison.

rate[36] known *star* integrals. Because Percus and Yevick have shown that the *graphs* contributing to the Percus–Yevick equation of state as derived from (26) are all *planar irreducible convex graphs*, we have obtained the virial coefficients through B_7 in this case by selecting

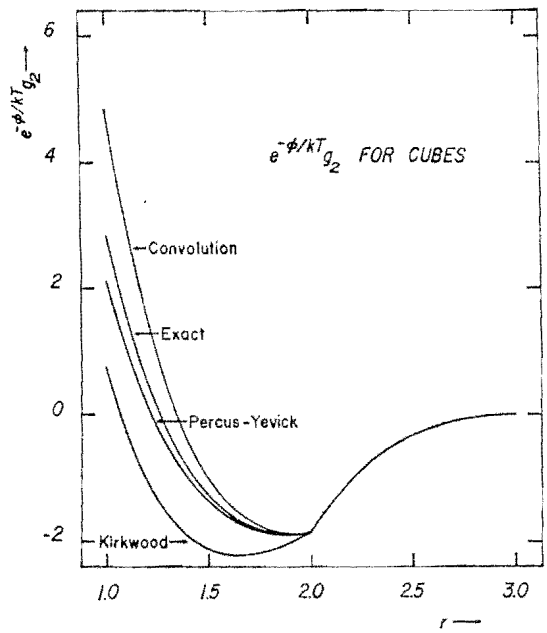

FIG. 7. $\mathrm{Exp}[-\phi(r)/kT]g_2(r)$ for hard cubes of unit volume according to three integral equations. The exact curve is included for comparison.

[36] Only in the case of the convolution and exact results is it possible to give a direct graphical representation (*lines* representing f functions only) of the equation of state as derived from the virial theorem. The theorem necessary to make this representation is given in G. S. Rushbrooke and H. I. Scoins, Proc. Roy. Soc. (London) **A216**, 203 (1953). See also Rushbrooke and Hutchinson.[33]

all such *graphs* from the list previously mentioned.[5] We have not evaluated $g_4(r)$ (numerically) for any of the three approximate integral equations. The task of evaluating the related *six-point doubly rooted graphs* is fairly tedious.

For molecules having a pairwise-additive potential energy which is either zero or infinity, there is yet another way of obtaining the pressure from the distribution function $\mathcal{G}(\mathbf{r})$. For such molecules we have established[18] the following relation between the potential of mean force at zero separation and the virial coefficients:

$$\Psi(0)-\phi(0)\equiv -kT\ln\mathcal{G}(0)=kT\sum_{n=2}\frac{n}{1-n}B_n\rho^{n-1}. \qquad (33)$$

Equation (33) has an interesting graphical interpre-

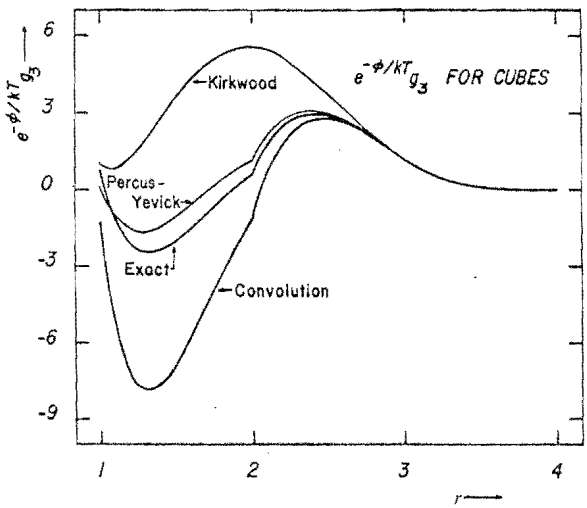

FIG. 8. $\mathrm{Exp}[-\phi(r)/kT]g_3(r)$ for hard cubes of unit volume according to three integral equations. The exact curve is included for comparison.

tation, the discovery of which actually led us to the equation. If one takes the *n-point graphs* which contribute to the potential of mean force (see Appendix I), and merges the *root points*, thus getting the potential of mean force at zero separation, the resulting $(n-1)$-*point graphs* are just those which contribute to the $(n-2)$nd irreducible cluster integral.[2] In the process of moving the *root points* together some *lines* become double *lines*, and to correct for this one must add an extra factor of -1 to the resulting *graph* for each pair of doubled *lines*. To illustrate these ideas we demonstrate in Table XIV how the *doubly rooted graphs* of *five points* which contribute to the potential of mean force generate the *star graphs* of *four points* as the *root points* are merged.

Returning to our Kirkwood example again we find from (21)–(23) that at zero separation the following

TABLE VIII. Virial coefficients for hard lines. The molecular side length is unit volume.

	From the Ornstein–Zernicke relation				From the virial theorem		
	B_4	B_5	B_6	B_7	B_4	B_5	B_6
Percus–Yevick	1.00000	1.00000	1.00000	1.00000	1.00000	1.00000	
Kirkwood	1.08333	1.20278			0.75000	0.61111	
Convolution	0.91667	0.80000	0.70278		1.50000	1.83333	2.00000
Exact	1.00000	1.00000	1.00000	1.00000	1.00000	1.00000	1.00000

equation holds:

$$\Psi(0)-\phi(0)$$

$$=kT\left\{\rho\int -d\mathbf{r}_2+\tfrac{1}{2}\rho^2\int \triangle\, d\mathbf{r}_2 d\mathbf{r}_3 + \tfrac{1}{6}\rho^3\int [3\square+5\boxtimes]d\mathbf{r}_2 d\mathbf{r}_3 d\mathbf{r}_4\right\}$$

$$=kT[-2\rho B_2-\tfrac{3}{2}\rho^2 B_3-\tfrac{4}{3}\rho^3 B_4]. \qquad (34)$$

Thus for squares

$$B_4=-\tfrac{1}{8}\int [3\square+5\boxtimes]d\mathbf{r}_2 d\mathbf{r}_3 d\mathbf{r}_4$$

$$=-\tfrac{1}{8}[3(16/3)^2-5(14/3)^2]=53/18.$$

In this way we can find B_3 and B_4 for the approximate integral equations (B_2 is given exactly by all three equations). We list the B_3, B_4 results in Tables XI–XIII. Both the Percus–Yevick and convolution integral equations fail to give correct third virial coefficients [using (33)], while the Kirkwood virial coefficients are generally closer to the exact values than those obtained from the Ornstein–Zernicke relation and the virial theorem. This suggests that (33) may be useful in getting thermodynamic quantities from integral equations,[37] although this simple form is obtained only when the molecules are hard.

We have noticed a relation similar to that illustrated in Table XIV among the *star graphs* themselves. We do not yet have a thermodynamic interpretation for this relation: removal of *point number n*, together with the *lines at that point*, from the set of *labeled stars* of n *points*, generates $n-2$ sets of the *labeled stars* of $n-1$ *points*. This last operation is illustrated in Table XV; a proof is given in Appendix III. Again one has to be careful about the sign of the derived *graphs*, and the physical interpretation of the operation would presumably hold for hard molecules only.

5. DISCUSSION AND CONCLUSION

We must restrict our comments here to the density region in which our number density expansions of the pressure and radial distribution function are useful. It is at least possible that some of the *graph*-type-selection or integral equation approximations we have treated are valid at (i) extremely low densities where only the second virial coefficient contributes significantly to the pressure, and at (ii) high densities near closest packing; and that we have had the misfortune of making comparisons only in an intermediate density range.

With regard to virial coefficient approximations of the *ring* and *watermelon* type, it has been pointed out by Salpeter[38] that such approximations may be particularly useful for long-range potentials. For the potentials we have considered this is evidently not the case. The contributions of the *star* integrals to B_n increase (with n) so rapidly that if all of the contributions to B_n have the same sign

$$|\lim_{n\to\infty} B_n| = \infty.$$

It is only the fact that almost exactly half of the contributions are negative and half positive that results in a convergent virial series.[39] It is because of this extensive cancellation that approximations which neglect some *graphs* are inherently dangerous. There are many ways of classifying *graphs*, however, and it is entirely possible that some selective process exists which would be useful for the molecules we have considered. This fact is illustrated by the Percus–Yevick equation which discards most of the *star graphs* and yet is exactly correct in one dimension through at least the seventh virial coefficient calculated by the Ornstein–Zernicke

[37] Inserting (33) into various integral equations gives quite different results. Taking (i) the Percus–Yevick equation, (ii) the Kirkwood equation, (iii) the convolution equation, and (iv) the Born–Green–Yvon equation, and specializing to the hard sphere $\phi(r)$, one can get, respectively, (i) the ideal gas law, (ii) the exact relation $z/\rho=\exp[\mu^{\text{excess}}/kT]$, (iii) some integrals which we have not been able to evaluate, and (iv) an equation of state with the correct B_2, but all higher $B_n=0$. The analog of (33) for the triplet distribution function is

$$\Psi(\mathbf{r}_{123}=0)-\phi(\mathbf{r}_{123}=0)=2kT\sum_{1-n}^{n} B_n\rho^{n-1};$$

use of the Kirkwood superposition approximation multiplies the right-hand side of this relation by $\frac{3}{2}$.

[38] E. E. Salpeter, Ann. Phys. (N. Y.) **5**, 183 (1958).

[39] G. W. Ford, dissertation, University of Michigan, 1954.

TABLE IX. Virial coefficients for hard squares. The molecular area σ^2 is unit volume.

	From the Ornstein–Zernicke relation				From the virial theorem		
	B_4	B_5	B_6	B_7	B_4	B_5	B_6
Percus–Yevick	3.77778	4.23611	4.42000	4.48761	3.33333	3.05556	
Kirkwood	4.72222	7.01690			2.16667	1.80556	
Convolution	2.94444	1.80417	0.96500		5.66667	5.88889	2.80417
Exact	3.66667	3.72222	3.02500	1.65065	3.66667	3.72222	3.02500

relation and through at least the fifth virial coefficient calculated by the virial theorem. Comparison of the exact and Percus–Yevick $\mathcal{G}(r)$'s (both are given in Table V) indicates that the functional form of $g(r)$ for the Percus–Yevick equation is probably exact in one dimension. Thus the *graphs* omitted by the Percus–Yevick equation cancel in one dimension but not (as one can see from Tables VI and VII) in two or three dimensions. Furthermore $\mathcal{G}(r)$ is incorrect for $0<r<1$ in one dimension, leading to incorrect B_n from $\mathcal{G}(0)$ by (33).

One might expect to get more reliable distribution functions from more complicated integral equations such as the Kirkwood–Salsburg equation[40] (which we find, using the superposition approximation and the correct number density expansion of the fugacity, gives $B_2 \cdots B_4$ correctly); unfortunately this equation is so complicated that no other calculations have yet been based upon it.

A set of integral equations due to Poirier[41] is quite different from those which we have treated here. His second- and third-order theories result in a *ring* approximation to the radial distribution function in which the *lines* represent $-\phi(\mathbf{r})/kT$ rather than $\exp[-\phi(\mathbf{r})/kT]-1$. It is interesting that this approximation gives the Debye–Hückel results for dilute electrolyte solutions. Preliminary calculations indicate that Poirier's fourth order theory, in which the approximate distribution function is determined by several coupled integral equations, does not have a graphical interpretation; that is, there is no number density expansion for the solution of the fourth order equations. We plan to investigate these equations further.

It appears that the Born–Green–Yvon integral equation has no solution for hard squares or cubes. The basic difficulty is that the equation allows one to solve for a number density expansion of the gradient of $g(x, y, z)$, but after finding this "gradient" one sees that there is no function symmetric in x, y, and z from which it can be derived. Thus in the Born–Green–Yvon case we cannot even obtain an approximate solution; the underlying Kirkwood superposition approximation produces an equation without solutions.

We have found (see Figs. 3–8) that the Percus–Yevick equation is more satisfactory than the Kirkwood or convolution equations in representing the radial distribution function. Because this equation also has the simplest structure of those which we have considered it deserves further study. By contrast, even with the smoothing inherent in calculating $g_n(r)$ from $g_n(\mathbf{r})$, it is clear (see Figs. 3–8) that the Kirkwood and convolution equations represent rather crude approximations in our density range.

Even with the Percus–Yevick equation (with radial distribution functions not markedly different from the exact curve) we find, in two or three dimensions, rather unreliable virial coefficients with the (optimum) Ornstein–Zernicke relation. This sensitivity of thermodynamic properties to the precise form of the radial distribution function has been shown vividly in

TABLE X. Virial coefficients for hard cubes. The molecular volume σ^3 is unit volume.

	From the Ornstein–Zernicke relation				From the virial theorem		
	B_4	B_5	B_6	B_7	B_4	B_5	B_6
Percus–Yevick	12.88889	12.43403	9.20674	11.58167	8.44444	0.56944	
Kirkwood	20.92593	37.94250			3.00000	4.20370	
Convolution	6.62963	−6.93947	−2.21330		19.33333	−5.17361	−49.60366
Exact	11.33333	3.15972	−18.87963	−43.50543	11.33333	3.15972	−18.87963

[40] J. G. Kirkwood and Z. Salsburg, Discussions Farad. Soc. **15**, 28 (1953).
[41] J. C. Poirier, J. Chem. Phys. **26**, 1427 (1957).

TABLE XI. Virial coefficients for hard lines from the potential of mean force. The molecular side length is unit volume.

	Percus-Yevick	Kirkwood	Convolution	Exact
B_3	0.66667	1.00000	2.00000	1.00000
B_4	0.50000	0.91667	3.00000	1.00000

the case of the Lennard-Jones potential.[42] Our final conclusions concerning hard lines, squares, and cubes are somewhat negative, namely that even if one uses an integral equation which gives a reasonably accurate distribution function (e.g., the Percus–Yevick equation) the thermodynamics obtained from it is (in the intermediate density range) (i) internally inconsistent (e.g., Ornstein–Zernicke vs virial theorem vs mean force potential), and (ii) unreliable. At present Monte Carlo and molecular dynamics studies represent the most reliable routes to thermodynamics (at intermediate and high densities) from the intermolecular potential as well as the best checks on integral equation work.

6. ACKNOWLEDGMENTS

The authors wish to express their gratitude to Professor Thomas M. Gallie, Jr., for his cooperation and to the National Science Foundation for support in making IBM 7070 computing time available at the Duke University Digital Computing Laboratory. We would like to thank Mr. George A. Neece for making available his Simpson's rule integration program (used in a numerical verification of virial coefficients obtained from the Ornstein–Zernicke relation). Finally, we would like to thank Professor Andrew G. De Rocco of the University of Michigan TCG for his active encouragement and critical reading of the manuscript.

APPENDIX I

In this appendix we outline some graphical terminology for the benefit of the reader who is not familiar with one of the basic works on graph theory.[43] Much of this material is taken from the lecture notes

TABLE XII. Virial coefficients for hard squares from the potential of mean force. The molecular area σ^2 is unit volume.

	Percus-Yevick	Kirkwood	Convolution	Exact
B_3	0.66667	3.00000	6.00000	3.00000
B_4	0.33333	2.94444	11.33333	3.66667

TABLE XIII. Virial coefficients for hard cubes from the potential of mean force. The molecular volume σ^3 is unit volume.

	Percus-Yevick	Kirkwood	Convolution	Exact
B_3	−3.33333	9.00000	18.00000	9.00000
B_4	4.66667	6.62963	38.66667	11.33333

TABLE XIV. Graphical illustration of the relation between the potential of mean force and the irreducible *star* graphs. Merging the *root points* of the *five-point doubly rooted graphs* shown gives the indicated *four-point star graphs*.

		⊠	⧅	□
6		0	0	6
12		0	0	−12
12		0	12	0
6		0	6	0
6		0	6	0
3		0	0	3
12		0	−12	0
12		0	−12	0
12		0	−12	0
6		0	−6	0
6		0	−6	0
6		6	0	0
6		−6	0	0
3		0	3	0
12		0	12	0
6		0	6	0
6		−6	0	0
3		0	−3	0
6		6	0	0
1		−1	0	0
	Totals	−1	−6	−3

[42] R. W. Zwanzig, J. G. Kirkwood, K. F. Stripp, and I. Oppenheim, J. Chem. Phys. **21**, 1268 (1953). In this paper it is pointed out that a change of 2.6% in the distance scale of the radial distribution function changes the pressure (under certain conditions) by a factor of 10^3.

[43] D. König, *Theorie der Endlichen und Unendlichen Graphen* (Chelsea Publishing Company, New York, 1950); C. Berge, *Theorei des graphes et ses applications* (Dunod Éditeur, Paris, 1958). For applications to statistical mechanics see R. J. Riddell, dissertation, University of Michigan, 1951; G. W. Ford[39]; G. E. Uhlenbeck and G. W. Ford.[31]

TABLE XV. Graphical illustration of the relation between the *stars* of n and $n-1$ *points* for $n=5$. Shown is the number of times each type of *four-point connected graph* appears when the relation (defined in Appendix III) is applied to the set of *labeled five-point stars*.

		⊠	⧅	□	⧄	⧅	⊓
12		0	0	0	0	0	12
60		0	0	12	24	0	−24
10		0	0	6	0	−4	0
10		0	0	0	0	4	0
60		0	24	0	−24	0	12
30		0	6	−12	−12	0	0
30		6	−12	0	12	0	0
15		0	−12	3	0	0	0
10		−4	6	0	0	0	0
1		1	0	0	0	0	0
Totals		3	18	9	0	0	0

of Professor Frank Harary's Graph Theory course at the University of Michigan.

The many applications of graph theory have led to several names for the same concept. For example, *points* of a *graph* are also known as *nodes*, *vertices*, *junctions*, or *0-simplexes*. Synonyms for *line* include *arc*, *edge*, *branch*, *link*, *wire*, and *1-simplex*. The *graphs* themselves (which are sets of *points* with *lines* connecting pairs of these *points*) are called *networks*, *nets*, *patterns*, *configurations*, *figures*, *diagrams*, *linear graphs*, or *1-dimensional simplicial complexes*.

The following definitions are relevant to this paper:

(1) A *graph* is called *labeled* if the *points* of the *graph* are distinguished from one another in some way (commonly by labeling the *points* numerically: 1, 2, ···) independent of the structure of the *graph*. Otherwise the *graph* is *unlabeled*.

(2) A *graph* is *disconnected* if it is possible to divide the *points* of the *graph* into two or more sets, such that no *lines* of the *graph* connect *points* of any two different sets. If such a division is impossible the *graph* is *connected*. According to Mayer's terminology such a *connected graph* is *at least singly connected*.

(3) A *point* P_a of a *connected graph* is said to be an *articulation point* if it is true that removing P_a (together with the *lines* at P_a) from the *graph* leaves a *disconnected graph*.

(4) A *connected graph* having at least one *line* and no *articulation points* is called a *star*. Other terms for *star* include *block* and *at least doubly connected graph*.

(5) The *degree* of a *point* is the number of *lines* adjacent to it. A *ring graph* is a *star*, all *points* of which are of *degree* 2. A *watermelon graph* is a *star* of n *points*; 2 *points* are of *degree* 3 and $n-2$ *points are* of *degree* 2. A *complete graph* of n *points* has all *points* of *degree* $n-1$. A *nearly complete graph* is a *star* of $n>3$ *points*; 2 *points* are of *degree* $n-2$ and $n-2$ *points* are of *degree* $n-1$.

(6) A *doubly rooted graph* is a *graph* in which two *root points* are specially distinguished, in some way, from the rest. We restrict our interest to *connected doubly rooted graphs* with *root points labeled* 1 and 2 not directly *connected* by a *line*, such that were the missing *line* linking the *root points* added the *graph* would become or remain a *star*. According to Van Leeuwen *et al.* such *graphs* are *composite* if removal of both *root points* gives a *disconnected graph*; otherwise they are *nodal* or *elementary*, the former if there exists any *point* the removal of which gives a *disconnected graph*, otherwise the latter.[44] The *graphs* contributing to the radial distribution function may be *composite*, *nodal*, or *elementary*. Of these only the *nodal* and *elementary graphs* contribute to the potential of mean force.

(7) The *planar irreducible convex graphs* resulting from the Percus–Yevick integral equation used in conjunction with the Ornstein–Zernicke relation may be constructed in the following way: start with a *labeled ring graph* of n *points*; by adding 0, 1, ··· *lines connecting* the *points* of the *ring graph* construct all possible *graphs* with noncrossing *lines* (keeping the original *ring graph* on a plane). $B_n(\mathrm{PY}, \mathrm{OZ})$ is then the sum of the corresponding *star* integrals divided by $-n$.[7]

(8) A *cycle* is an ordered set of $k>2$ distinct *points* of a *graph*, $P_1, P_2, \cdots P_k$, such that P_j is *connected* to P_{j-1} and P_{j+1} for all j with the conventions $P_0 \equiv P_k$ and $P_1 \equiv P_{k+1}$.

APPENDIX II

In this appendix we show that the value of any one-dimensional (hard line) *star* integral of n *points* and $\binom{n}{2}$ *lines* is $(-)^{[n/2]}n$, and that the value[21] of any one-dimensional (hard line) *star* integral of n *points* and $\binom{n}{2}-1$ *lines* is $-(-)^{[n/2]}\{n+(2/[n-1])\}$. (Again we are using the units $\sigma \equiv 1$.) The integrals we are considering are volume-independent and have the form

$$I=(1/V)\int S_i(n)d\mathbf{r}_1\cdots d\mathbf{r}_n= \int_{\text{(molecule 1 at origin)}} S_i(n)d\mathbf{r}_2\cdots d\mathbf{r}_n. \tag{II.1}$$

[44] J. M. J. Van Leeuwen *et al.*[9]

We assume some familiarity with a previous paper in which the evaluation of one-dimensional integrals was described in detail.[5]

We recall that any *star* integral may be written as the sum of $n!$ subintegrals, one for each of the ways n molecules may be ordered from left to right. Thus the *star* integral contributing to B_3, $(1/V)\int\triangle d\mathbf{r}_1\cdots d\mathbf{r}_3$, may be written as the sum of six subintegrals corresponding to the 3! orderings 123, 132, 213, 231, 312, 321. In the event that the first and last molecules in a given ordering (of the *points* of any *star*) are connected by a *line* (in that *star*) one shows easily that the value of the corresponding subintegral is $\pm 1/(n-1)!$; the sign is determined by the number of *lines* in the *star*. This value for the subintegral is obtained because the restrictions of the ordering and the f function linking the first and last molecules restrict the integration to one of $n-1$ equal parts of an $(n-1)$-dimensional cube of side-length σ, the molecular length. We illustrate the case for $n=6$, using the ordering 123456 and assuming that f_{16} appears in the integrand.

σ subintegral

$$=\int_0^\sigma dw\int_w^\sigma dx\int_x^\sigma dy\int_y^\sigma dz\int_z^\sigma da$$

$$=\int_0^\sigma dw\int_w^\sigma dx\int_x^\sigma dy\int_y^\sigma dz(\sigma-z)/1!$$

$$=\int_0^\sigma dw\int_w^\sigma dx\int_x^\sigma dy(\sigma-y)^2/2!=\int_0^\sigma dw\int_w^\sigma dx(\sigma-x)^3/3!$$

$$=\int_0^\sigma dw(\sigma-w)^4/4!=\sigma^5/5!=1/5! \quad \text{(II.2)}$$

The general case is obvious from this illustration. If the *star* we consider is *complete* all orderings of the n molecules will give σ subintegrals, of value $\pm 1/(n-1)!$. Because $n!$ of these orderings are possible the value of the *star* integral corresponding to a *complete graph* is $\pm n$.

For a *star* with $\binom{n}{2}-1$ *lines* it is clear that all orderings in which the missing *line* is not between the first and last molecules will give σ subintegrals. The remainder of the orderings, $2(n-2)!$ in number, will contribute w subintegrals, which we represent schematically as follows:

w subintegral $=(1/V)\int$ 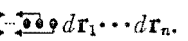 $d\mathbf{r}_1\cdots d\mathbf{r}_n$. (II.3)

Using the ordering 123456 and assuming that f_{16} does not appear in the integrand, we may evaluate a *six-point* w subintegral:

$$w \text{ subintegral}=\int_0^\sigma dw\int_w^\sigma dx\int_x^\sigma dy\int_y^\sigma dz\int_z^{\sigma+w} da$$

$$=\sigma \text{ subintegral}+\int_0^\sigma dw\int_w^\sigma dx\int_x^\sigma dy\int_y^\sigma dz\int_\sigma^{\sigma+w} da. \quad \text{(II.4)}$$

Integrating by parts over w (following the integrations over $a\cdots x$) we see that the last integral in (II.4) has the same value as a σ subintegral. Thus the w subintegral has value $\pm 2/(n-1)!$, and the value of a *star* integral with $\binom{n}{2}-1$ *lines* and n *points* is (apart from sign)

$$\frac{n!-2(n-2)!}{(n-1)!}+\frac{2(2)(n-2)!}{(n-1)!}=n+\frac{2}{n-1}.$$

All that remains is to determine the sign of the integrals. We observe that

$$(-)^{\binom{n}{2}}=(-)^{[n/2]},$$

giving the sign of the *complete graph* integral. The sign of the *graph* obtained by removing one *line* from a *complete graph* is necessarily opposite, being $-(-)^{[n/2]}$.

APPENDIX III

In this appendix we state and prove a graph-theoretical theorem which presumably has (unknown) thermodynamic implications. In this appendix we will be concerned with *labeled graphs* only.

Let us denote the set of *labeled stars* of n *points*, $P_1\cdots P_n$, by $\mathfrak{S}(n)$, and the set of *labeled connected graphs* of n *points* which are not *stars* by $\mathfrak{C}(n)$. Particular *graphs* in these sets will be indicated by $S_k(n)$ and $C_k(n)$ respectively. We define a general relation between pairs of *labeled graphs*, $G_1(n)$ and $G_2(n-1)$, by writing

$$G_1(n)\rightarrow\pm G_2(n-1) \quad \text{(III.1)}$$

if (and only if) it is true that removing P_n and all *lines* joining $P_1\cdots P_{n-1}$ to P_n from $G_1(n)$ leaves $G_2(n-1)$. If the number of *lines* removed is even (odd) we use a plus (minus) sign in (III.1). The following pairs of *graphs* satisfy the relation, where $P_n=P_5$ is the topmost *point* in the *five-point graphs* shown.

Using our notation we wish to prove the following:

$$\mathfrak{S}(n)\rightarrow[n-2]\mathfrak{S}(n-1). \quad \text{(III.2)}$$

Because removing a single *point* from a *star* never results in a *disconnected graph*, we may divide the set of *stars* of n *points* into two sets: $\mathfrak{S}_s(n)$, those *stars* which

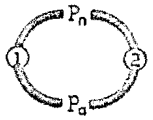

FIG. 9. A schematic representation of $G_k^*(n)$, a *graph* formed by removing the *line* P_a-P_n from an element $G_k(n)$ of $\mathfrak{S}_k(n)$.

give *stars* of $n-1$ *points* on removal of P_n; and $\mathfrak{S}_c(n)$, those *stars* which give *connected graphs* of $n-1$ *points* which are not *stars*. Evidently $\mathfrak{S}_s(n) \cup \mathfrak{S}_c(n) = \mathfrak{S}(n)$.

Consider $\mathfrak{S}_s(n)$. For a particular $S_k(n-1)$ there is one *star* in $\mathfrak{S}_s(n)$ in which P_n is linked to $S_k(n-1)$ by $n-1$ *lines*; there are $n-1$ *stars* in $\mathfrak{S}_s(n)$ in which P_n is linked to $S_k(n-1)$ by $n-2$ *lines*, and in general exactly $\binom{n-1}{n-1-j}=\binom{n-1}{j}$ *stars* in $\mathfrak{S}_s(n)$ which give $(-)^j S_k(n-1)$ for $1<j<n$. *Graphs* which consist of $S_k(n-1)$ joined to P_n by a single *line* are clearly not *stars* and will therefore not appear in $\mathfrak{S}_s(n)$. Thus the number of times that $S_k(n-1)$ will appear in the *stars* derived from $\mathfrak{S}_s(n)$ [by removal of P_n according to (III.1)] is, independent of k,

$$\sum_{j=2}^{n-1}(-)^j\binom{n-1}{j}=\sum_{j=0}^{n-1}(-)^j\binom{n-1}{j}-\sum_{j=0}^{1}(-)^j\binom{n-1}{j}$$
$$=0-[1-(n-1)]=n-2. \quad \text{(III.3)}$$

Because each *star* in $\mathfrak{S}_s(n)$ will give some $S_k(n-1)$ on removal of P_n, and because each $S_k(n-1)$ is obtained exactly $n-2$ times from $\mathfrak{S}_s(n)$ we find

$$\mathfrak{S}_s(n) \rightleftharpoons [n-2]\mathfrak{S}(n-1). \quad \text{(III.4)}$$

We now consider $\mathfrak{S}_c(n)$. For a particular $C_k(n-1)$ containing the *articulation point* P_a we may select from $\mathfrak{S}_c(n)$ two sets of *stars*: $\mathfrak{S}_k(n)$, those *stars* in $\mathfrak{S}_c(n)$ which have the *line* joining P_a to P_n and give $C_k(n-1)$ when P_n is removed; $\mathfrak{S}_k^*(n)$, those *stars* in $\mathfrak{S}_c(n)$ which do not have the *line* joining P_a to P_n and give $C_k(n-1)$ when P_n is removed. We now demonstrate that there is a one-to-one correspondence between the *stars* in $\mathfrak{S}_k(n)$ and the *stars* in $\mathfrak{S}_k^*(n)$. For any *star*

TABLE XVI. B_4 according to the Ornstein–Zernicke relation from three integral equations, and according to the virial theorem from the convolution equation. The number of times each *graph* contributes to the integrand in

$$B_4=(-1/8V)\int(4\text{-}point\ graphs)d\mathbf{r}_1\cdots d\mathbf{r}_4$$

is given in this table.

	PY(OZ)	K(OZ)	C(OZ)	C(VT)
□	2	3	3	3
⊠	4	4	5	6
⊠	0	−1	0	0

TABLE XVII. B_5 according to the Ornstein–Zernicke relation from three integral equations, and according to the virial theorem from the convolution equation. The number of times each *graph* contributes to the integrand in

$$B_5=(-1/30V)\int(5\text{-}point\ graphs)d\mathbf{r}_1\cdots d\mathbf{r}_5$$

is given in this table.

	PY(OZ)	K(OZ)	C(OZ)	C(VT)
⬠	6	12	12	12
⬟	30	36	48	60
⬠	30	25	42	60
⊠	0	4	7	10
⊠	0	5	7	10
⊠	0	−6	0	0
⊠	0	−7	0	0
⊠	0	−3	0	0

TABLE XVIII. B_6 according to the Ornstein–Zernicke relation from the Percus–Yevick and convolution integral equations, and according to the virial theorem from the convolution equation. The number of times each *graph* contributes to the integrand in

$$B_6=(-1/144V)\int(6\text{-}point\ graphs)d\mathbf{r}_1\cdots d\mathbf{r}_6$$

is given in this table.

	PY(OZ)	C(OZ)	C(VT)
⬡	24	60	60
⬡	144	288	360
⬡	72	132	180
⬡	0	120	180
⬡	0	120	180
⬡	0	9	15
⬡	288	480	720
⬡	144	240	360
⬡	72	120	180
⬡	0	216	360
⬡	0	9	15
⬡	0	216	360
⬡	48	72	120
⬡	144	216	360
⬡	144	216	360

in $\mathfrak{S}_k^*(n)$ there is a corresponding *star* in $\mathfrak{S}_k(n)$, identical but for the presence of the *line* P_a-P_n joining P_a to P_n. This follows from the observation that adding a *line* to the *points* of a *star* always gives another *star*. To establish that for any *star* in $\mathfrak{S}_k(n)$ there is a corresponding *star* in $\mathfrak{S}_k^*(n)$, identical but for the absence of the *line* P_a-P_n, is somewhat more tedious. This demonstration is equivalent to showing that any two *points* in $G_k^*(n)$, a *graph* formed by removing the *line* P_a-P_n from an element $G_k(n)$ of $\mathfrak{S}_k(n)$, lie on a *cycle*. Let us consider two *points* P_b, P_c, other than P_a or P_n in $G_k^*(n)$ and draw $G_k^*(n)$ as in Fig. 9, where ① and ② represent two of the two or more *connected graphs* formed by removal of P_a and P_n from $G_k^*(n)$. Without loss of generality we suppose P_b is in ①, and P_c is in either ① or ②. If P_c is in ② any *cycle* on which both P_b and P_c lay in $G_k(n)$ is also in $G_k^*(n)$, because such a *cycle* could not include the *line* P_a-P_n. If both P_b and P_c are in ① any *cycle* on which both lay in $G_k(n)$ is also in $G_k^*(n)$ unless the *cycle* included P_a-P_n. In the latter case we can construct a new *cycle* in $G_k^*(n)$ by replacing the $G_k(n)$ *cycle* with a *cycle* identical to it but for the substitution of any path through ② from P_a to P_n for the *line* P_a-P_n. In this way we have shown that any two *points* (other than P_a and P_n) which lay on a *cycle* in $G_k(n)$ lie on a *cycle* in $G_k^*(n)$, and that $G_k^*(n)$ is therefore a *star* corresponding to $G_k(n)$, provided only that we show P_a and P_b, P_a and P_c, P_b and P_n, P_c and P_n also lie on *cycles* in $G_k^*(n)$. These facts are all easily shown in the foregoing manner, and the one-to-one correspondence between the *stars* in $\mathfrak{S}_k(n)$ and the *stars* in $\mathfrak{S}_k^*(n)$ is established. We illustrate it here, for a particular case, taking  as the particular *labeled* $C_k(5)$, indicating the *articulation point* P_a by an open circle.

$\mathfrak{S}_k^*(6)=\{$  ,  $\}$ and $\mathfrak{S}_k(6)=\{$,  $\}$.

Noting again that

$$\bigcup_k \{\mathfrak{S}_k(n) \cup \mathfrak{S}_k^*(n)\}=\mathfrak{S}_c(n),$$

and observing that

$$\{\mathfrak{S}_k(n) \cup \mathfrak{S}_k^*(n)\} \not\simeq \varnothing,$$

where $\varnothing$ is the empty set, we have the result

$$\mathfrak{S}_c(n) \not\simeq \varnothing. \qquad \text{(III.5)}$$

Taking the union of (III.4) and (III.5) gives (III.2), and completes the proof.

APPENDIX IV

In this appendix we catalog graphical expressions for virial coefficients obtained from the Percus–Yevick, Kirkwood, and convolution integral equations using (i) the Ornstein–Zernicke relation, (ii) the virial theorem, and (iii) the potential of mean force at zero separation.[45] Tables XVI–XVIII give $B_4\cdots B_6$ calculated from (i) for all[46] three integral equations and from (ii) for the convolution equation. We have used an expression for B_7 only in the case of the Percus–Yevick equation as applied to the Ornstein–Zernicke relation; this expression for B_7(PY, OZ) is given by (IV.1). Finally, in (IV.2) and (IV.3) we give B_3 and B_4 as obtained from the potential of mean force at zero separation for each of the three integral equations:

B_7(PY, OZ)

$$=(-1/840V)\int[120\,\text{  }+840\,\text{  }+840\,\text{}+1680\,\text{}$$

$$+840\,\text{  }+840\,\text{  }+840\,\text{}+1680\,\text{  }+840\,\text{  }+840\,\text{  }$$

$$+1680\,\text{  }+1680\,\text{  }+1680\,\text{}+1680\,\text{}+1680\,\text{  }$$

$$+840\,\text{}+1680\,\text{  }+1680\,\text{}+840\,\text{}+840\,\text{  }]$$

$$\times d\mathbf{r}_1\cdots d\mathbf{r}_7. \qquad \text{(IV.1)}$$

$B_3[\Psi(0)\,(\text{PY, K, C})]$

$$=(-1/3V)\int[(2,1,2)\,\triangle+(1,0,0)\,\wedge]d\mathbf{r}_1\cdots d\mathbf{r}_3. \qquad \text{(IV.2)}$$

$B_4[\Psi(0)\,(\text{PY, K, C})]$

$$=(-1/8V)\int[(6,3,6)\,\square+(12,5,12)\,\text{}$$

$$+(6,0,0)\,\text{}+(2,0,0)\,\text{}]d\mathbf{r}_1\cdots d\mathbf{r}_4.^{47} \qquad \text{(IV.3)}$$

[45] In the case of the Percus–Yevick and Kirkwood integral equations, the theorem of Rushbrooke and Scoins[36] is not useful.

[46] We have not calculated B_6 from the Kirkwood equation according to the Ornstein–Zernicke relation.

[47] The exact expressions in terms of *graphs* are given in reference 5 for $B_2\cdots B_7$, including the 448 *seven-point stars* not appearing in (IV.1) which contribute to the exact B_7.